ELSEVIER

Ceramics International 29 (2003) 713–719

CERAMICS INTERNATIONAL

www.elsevier.com/locate/ceramint

Erosion characteristics of silicon nitride ceramics

Hyeon-Ju Choi[a], Dong-Ho Han[b], Dong-Soo Park[c,*], Hai-Doo Kim[c], Byung-Dong Han[c], Dae-Soon Lim[a], Il-Soo Kim[b]

[a]*Department of Materials Science and Engineering, Korea University, Anam-dong, Sungbuk-ku, Seoul, South Korea*
[b]*Department of Advanced Materials Engineering, Dong-eui University, Kaya-dong, Pusanjin-ku, Pusan, South Korea*
[c]*Ceramic Materials Group, Korea Institute of Machinery and Materials, 66 Sang-Nam-Dong, Chang-Won City, Kyong-Nam, South Korea*

Received 15 September 2001; received in revised form 12 March 2002; accepted 14 November 2002

Abstract

Silicon nitride ceramics with three different microstructures were prepared using three different silicon nitride powders and β-silicon nitride whiskers in order to study their erosion characteristics. Samples with a coarse microstructure were prepared by using a commercially available silicon nitride powder seeded with the whiskers. Samples with fine microstructures were obtained using fine silicon nitride powders that had been milled in toluene or in distilled water. The powder milled in toluene gained both carbon and oxygen during milling. Heating the powder at 1673 K for 10 h in a flowing nitrogen atmosphere reduced carbon and oxygen contents to the level of as-received powder. The powder milled in distilled water gained a significant amount of oxygen during milling, and silicon oxynitride (Si_2N_2O) was detected by X-ray diffraction analysis (XRD) from the sample sintered with it. The sample sintered with the powder milled in distilled water showed the finest microstructure and the lowest erosion rate among the samples. Erosion occurred mainly by dislodgment of grains.

Keywords: B. Grain size; B. Microstructure; D. Silicon nitride; Erosion; Silicon oxynitride

1. Introduction

Silicon nitride has been widely studied due to its good and well-balanced properties [1–3]. Silicon nitride is a material difficult to machine [2], which suggests that it can perform well in wear applications. In fact, silicon nitride is widely used for making cutting tools, bearings and other wear parts. In some applications like sand blast nozzles and abrasive water jet nozzles, erosion is the major wear mechanism causing deterioration of a part. There are a number of reports describing the erosion of silicon nitride and its solid solution, SiAlON [2,4–6]. These studies found that the erosion resistance of silicon nitride did not exhibit the dependence on the fracture toughness as predicted by the model based on brittle fracture mechanics [6]. The erosion rate of alumina was reported to be proportional to $G/(G+G_o)$, where G and G_o are grain size and characteristic grain size, respectively [7]. The main erosion mechanism for Si_3N_4 or Al_2O_3 was grain detachment following crack propagation along a low energy grain face that, in most cases, is a grain boundary. It seems reasonable to expect a better erosion resistance for silicon nitride with a finer microstructure. One of the ways to make silicon nitride with fine microstructure is to use fine starting powder. Intensive milling is a useful method for reducing the particle size. In the present study, silicon nitride ceramics with three different microstructures were prepared from a commercially available silicon nitride powder and intensively milled powders in order to examine their erosion characteristics.

2. Experimental

β-Silicon nitride whiskers (SN-WB, Ube Industries Ltd., Tokyo, Japan) were classified by air classification method into three size groups, and only the coarse fraction was used for seeding. Average length and width of the seeds were obtained from measuring 520 whiskers using an image analysis software (Image-Pro 3.0, Media

* Corresponding author.
E-mail address: pds1590@kmail.kimm.re.kr (D.-S. Park).

0272-8842/03/$30.00
doi:10.1016/S0272-8842(02)00222-5

Cybernetics, L.P., Silver Spring, MD, USA). Mean particle size of as-received silicon nitride powder (SN E10, Ube Industries Ltd.) was obtained using a particle size analyzer (SALD-2001, Shimadzu, Tokyo, Japan). Samples with a coarse microstructure (named as sample C) were prepared with 92 wt.% silicon nitride powder, 6 wt.% yttria (grade C, H.C. Starck Co., Berlin, Germany), 1 wt.% alumina (AKP-30, Sumitomo Chemical Co., Osaka, Japan) and 1 wt.% β-Si_3N_4 seeds. The powders, without the seeds, were mixed for 7 h using a planetary ball mill. Mixing was stopped for the seed addition and was resumed for 1 h. A monocast nylon jar, silicon nitride balls with 5 mm in diameter and ethanol were used for mixing. The powder mixture was pressed into 35×35×7 mm^3 plates using 20 MPa in a lever press, and then cold isostatically pressed at 250 MPa in an evacuated latex tubing. The pressed samples were packed with silicon nitride–boron nitride powder mixture in a graphite crucible, and was sintered at 2173 K for 4 h under 2.3 MPa nitrogen pressure.

As-received silicon nitride powder was intensively milled at 150 rpm in the planetary ball mill for 20 h using a silicon nitride jar with 8 times as much silicon nitride balls as the powder either in toluene or in distilled water. The specific surface area of silicon nitride powder before and after the intensive milling was measured using single point BET method. Oxygen content and carbon content of the powder before and after milling were measured using oxygen analyzer (TC-136, LECO Co., St. Joseph, MI, USA) and carbon analyzer (CS-344, LECO Co.), respectively. The powder milled in toluene was pressed into a disk of 36 mm diameter by 5 mm thick at 20 MPa using a lever press. The pressed sample was heated to 1673 K for 10 h in a flowing nitrogen atmosphere for decreasing its carbon and oxygen contents. After the heat treatment, the compact was crushed and ground by hand using an agate mortar and pestle. The ground powder was mixed with 6 wt.% yttria and 1 wt.% alumina for 8 h using a planetary ball mill for making sample FC. Mixing was performed for 8 h in a planetary ball mill as for sample C, but without the seed addition. The powder milled in distilled water was mixed with 6 wt.% yttria and 1 wt.% alumina to make sample FW. Mixing was performed in the same way as for samples C and FC. Samples FC and FW were prepared by hot pressing the powder mixture at 2023 K for 1 h under 30 MPa pressure in a flowing nitrogen environment using a boron nitride coated graphite punch and mould.

Density of the samples was measured using water immersion method. X-ray diffraction analysis was performed on the surface of sintered sample after grinding. Samples were ground and polished with 1 μm diamond slurry. Vickers hardness and the fracture toughness using indentation crack length method [8] were measured using 9.8 N and 196 N loads, respectively. Polished samples were plasma etched using 90% O_2–10% CF_4 gas mixture. Grain size measurement was performed on SEM micrographs of the etched samples using an image analysis software. At least 500 grains were measured for each sample. Samples were cut into 15×25×3 mm^3 plates and the two large surfaces were polished with 1 μm diamond slurry for the erosion tests.

Erosion test was performed using a gas-blast type equipment shown schematically in Fig. 1. The impacting abrasives were 150 mesh SiC particle (average particle size: 130 μm). The incident angle was fixed at 90° and the spacing between the sample and the 3 mm diameter nozzle was 10 mm. The tests were performed at room temperature, 573 K, 773 K and 973 K for about 15 min, a time in which 200 g of abrasive was consumed. The abrasive was heated while passing through the pipe inside the furnace as shown in Fig. 1. Weight change of the sample at the completion of the test was measured using a precision balance with 10 μg sensitivity. Erosion rate was obtained by the weight loss of the sample divided by weight of the impacting abrasives. Each test was repeated three times and average erosion rate was obtained. The eroded area was observed using SEM equipped with field emission gun (FEG-SEM) after gold coating to avoid electron charging.

3. Results and discussion

Average length and width of the whisker seeds were 16.94 μm and 2.76 μm, respectively, and mean particle size of as-received silicon nitride powder was 0.6 μm. While as-received silicon nitride powder contains 1.8 wt.% oxygen, the oxygen contents of the powders milled in toluene and in distilled water were 4.5 wt.% and 6 wt.%, respectively. Carbon contents were also changed from 0.19 wt.% to 2.1 wt.% and to 0.16 wt.% after milling in toluene and in distilled water, respectively. The increase of oxygen and carbon during ball milling in several solvents including water and ethanol has been reported [9]. According to the report, oxygen content of silicon nitride powder was increased due to oxidation during milling, and it was increased more as the solvent contains more oxygen. In case of toluene, there is no oxygen in its chemical formula ($C_6H_5CH_3$). Toluene used in this study was informed to have only 2 ppm water. Therefore, the large increase in oxygen content of the powder milled in toluene was not mainly due to oxidation during milling.

Another reason for the increase of oxygen content of the powder after milling was the increased surface area of the powder due to reduction of the particle size. If thickness of the oxide layer was independent of the particle size, oxygen content of silicon nitride powder was increased as the specific surface area was increased. The specific surface area of as-received silicon nitride

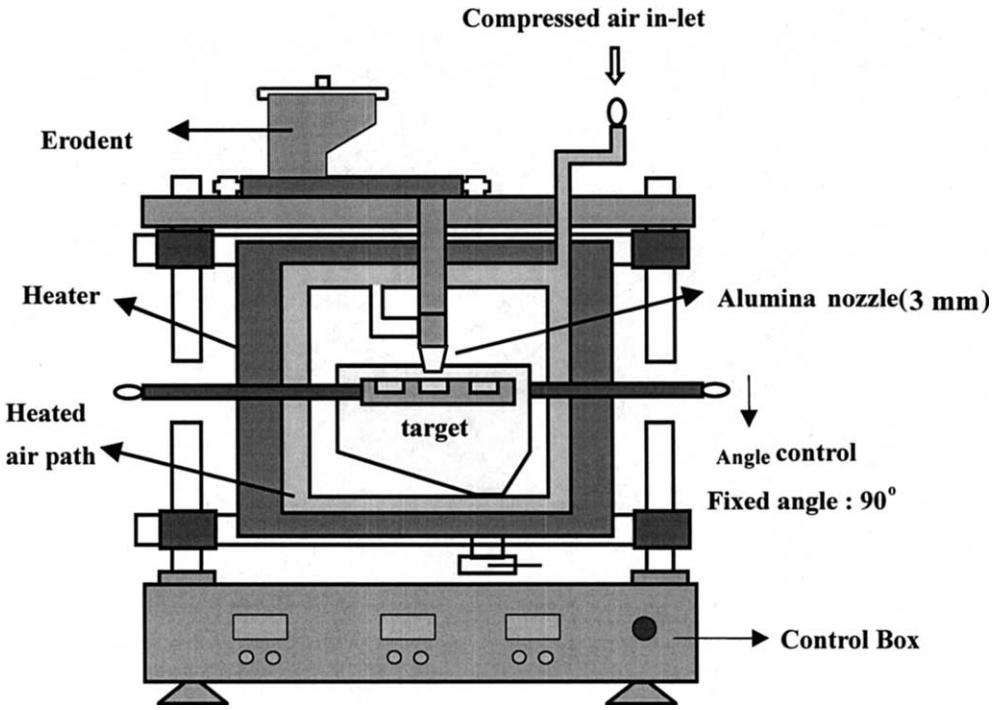

Fig. 1. Schematic diagram of high temperature erosion tester.

powder was 11.7 m^2/g while that of the powder milled in tolune was 30.8 m^2/g. Ratio of oxygen content of as-received silicon nitride powder to that of the powder after milling was 1/2.5 and was close to the ratio between the specific areas of the two powders. Therefore, the increase of oxygen content of silicon nitride powder after milling in toluene was mainly due to increase of total surface area of the powder. In case of the powder milled in water, the oxygen content was increased more than three times (from 1.8 wt.% to 6 wt.%) while the specific area was increased from 11.8 m^2/g to 25.9 m^2/g. Oxidation of the powder during milling in distilled water played an important role in increasing its oxygen content. Increase of carbon content of silicon nitride powder milled in toluene was mainly caused by the tribo-chemical reaction between the powder and toluene as reported for silicon nitride powder milled in cyclohexane [9]. Heating silicon nitride powder milled in toluene at 1673 K for 10 h in a flowing nitrogen environment reduced oxygen content of the powder to 1.88 wt.% and the remaining carbon content to 0.15 wt.%. The heat treatment temperature was high enough for hard agglomerates of particles to be formed and the specific surface area of the powder was decreased from 30.8 m^2/g to 18.3 m^2/g after the heat treatment.

Density of sintered samples were greater than 99% TD. Fig. 2 shows that only β-silicon nitride was detected from samples C and FC while silicon oxynitride (Si_2N_2O) as well as β-silicon nitride was detected from sample FW. In case of hot-pressed samples, the XRD patterns were obtained from the surface normal to the pressing direction. That is the reason why (101) peak in the patterns of the hot-pressed samples (samples FC and FW) was weaker than that in the pattern of gas pressure sintered sample (sample C). In other words, the elongated grains in the hot-pressed samples were not randomly oriented as those in the gas pressure sintered sample. A significant portion of the elongated grains were lying on the plane normal to the pressing direction (see Fig. 3). Sample C contained large reinforcing grains in a fine-grained matrix. The microstructure of sample FC is much finer than sample C, and sample FW has finer microstructure than sample FC. Even though the XRD patterns of sample FW indicates that silicon oxynitride is present in the sample, it is hard to be recognized from the microstructure shown in Fig. 3(c). Si_2N_2O was reported to have elongated morphology similar to that of β-silicon nitride grains [9]. Growth of the elongated silicon oxynitride grains was reported to improve the fracture toughness of silicon nitride ceramic composite [10]. Table 1 shows that average grain widths of samples C, FC and FW. One of the reasons for bigger grain size for sample FC than for sample FW is that the starting powder for the sample FC was heat treated at 1673 K for 10 h prior to sintering. Vickers hardness and the fracture toughness of the samples are also shown in Table 1. The highest fracture toughness of sample C among the three samples resulted from the coarse microstructure. It is interesting to find that sample FW showed higher fracture toughness than sample FC although the former had finer microstructure than

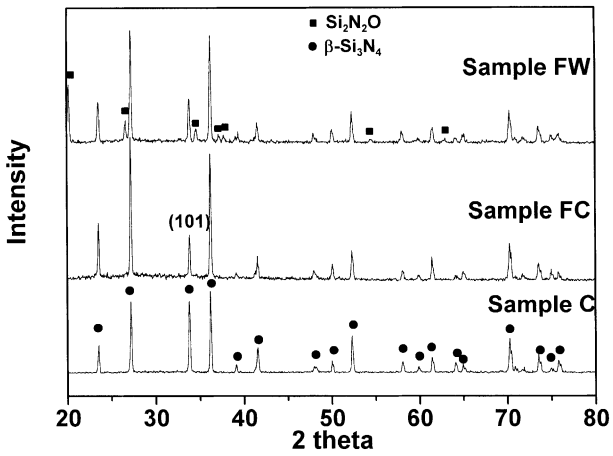

Fig. 2. XRD patterns of samples.

the latter. It is explained in part by presence of Si_2N_2O in sample FW. Si_2N_2O was reported to increase the fracture toughness of Si_3N_4–Si_2N_2O composite [11].

Fig. 4 shows the erosion rates of the samples as a function of the test temperature. Erosion rate of the sample was increased as the temperature was increased. Also, erosion rate of sample C was the highest at all the test temperatures while that of sample FW the lowest among the samples. According to the model proposed by Evans et al., the erosion rate is proportional to $Kc^{-1.3}$ times $H^{-0.25}$ [12]. However, the erosion rates of the samples shown in Fig. 4 can not be explained by that model. In fact, the erosion rate of sample C should have been lower than that of the other samples according to the model. Fig. 5 shows the erosion rates of the samples plotted as an inverse of the grain size, and shows that the erosion rate decreased as the grain size decreased This relationship suggests that the erosion rates of the samples were more dependent on the microstructure than on the mechanical properties as described by Davidge and Riley [7]. Fig. 6(a)–(f) shows eroded areas of the samples tested at room temperature and at 973 K. Fig. 6(a)–(c) shows that the major material removal mechanism at room temperature was micro-fracture followed by grain dislodgment as indicated by arrow in Fig. 6(a). A layer consisting of very fine particles smeared part of the area where grain dis-

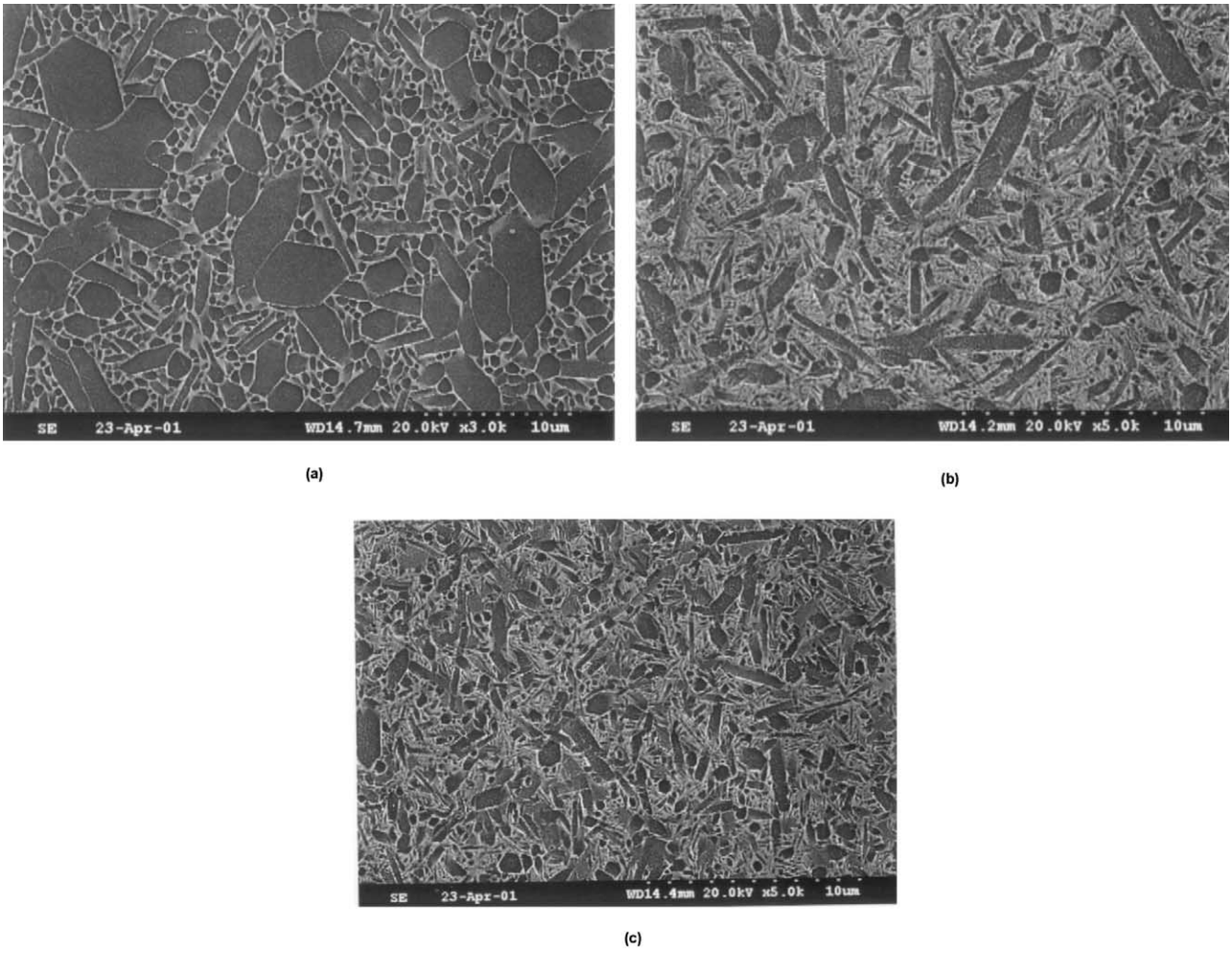

Fig. 3. FEG-SEM micrographs of plasma etched samples; (a) sample C, (b) sample FC and (c) sample FW.

Table 1
Summary of fabrication, phase characteristics, mechanical properties and erosion results

Sample	Fabrication	Phase	Grain size	Mechanical properties	Erosion rate ($\times 10^{-5}$ g/g)
C	Mixing (As-received powders + whiskers)−GPS at 2173K for 4h	β-Si_3N_4	2.51 μm	σ_{3p} = 664±87 MPa Hv = 14.2±0.3 GPa K_{IC} = 4.9±0.2 MPam$^{1/2}$	298K: 6.7±0.1 573K: 8.3±0.3 773K: 13.5±0.9 973K: 13.4±0.3
FC	Intensive milling (Si_3N_4 powder) in toluene–mixing–HP at 2023K for 1h	β-Si_3N_4	0.63 μm	σ_{3p} = 1108±88 MPa Hv = 15.3±0.1 GPa K_{IC} = 4.3±0.1 MPam$^{1/2}$	298K: 4±0.1 573K: 6.4±0.2 773K: 8.2±0.1 973K: 11.3±1.0
FW	Intensive milling (Si_3N_4 powder) in water–mixing–HP at 2023K for 1h	β-Si_3N_4 + Si_2N_2O	0.51 μm	σ_{3p} = 1085±61 MPa Hv = 15.3±0.1 GPa K_{IC} = 4.6±0.1 MPam$^{1/2}$	298K: 2.5±0.2 573K: 5.2±0.6 773K: 7.5±1.4 973K: 8.4±0.5

lodgment occurred. Also, localized plastic deformation caused by repeated impact of the eroding particles was observed on the eroded surface. As the test temperature was increased, grain dislodgment occurred more severely and the eroded surface became rougher. Sample C had the roughest eroded area and sample FW the smoothest among the samples. Comparing the grain width, hardness and fracture toughness values of samples FC and FW, the difference in the erosion rates of those two samples should not be as great as that shown in Table 1. The reason for such a big difference is not clear at this point. It implies a possibility for Si_2N_2O to have better erosion resistance than Si_3N_4. Further study on the effect of Si_2N_2O on the erosion rate of Si_3N_4–Si_2N_2O composites is being carried out.

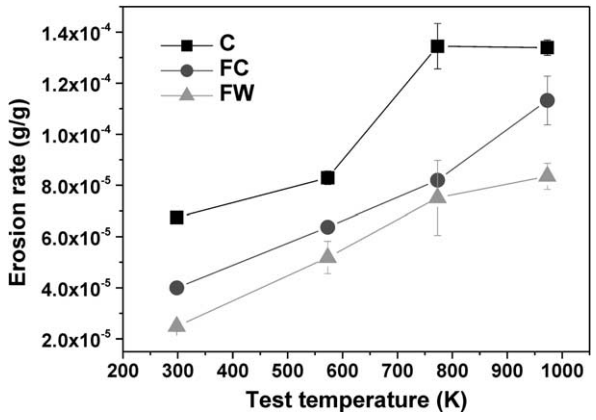

Fig. 4. Erosion rates of samples according to the test temperature.

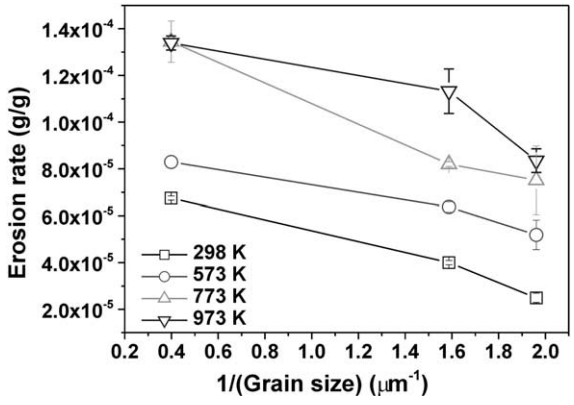

Fig. 5. Erosion rates vs. inverse of grain width; symbols represent different test temperatures.

4. Summary

Silicon nitride ceramics with three different microstructures were prepared with 6 wt.% yttria and 1 wt.% alumina as sintering additives using a commercially available silicon nitride powder with 1 wt.% of coarse silicon nitride whisker seeds and intensively milled silicon nitride powders. Carbon content as well as oxygen content of silicon nitride powder was increased by the intensive milling in toluene, while only the oxygen content was increased by more than three times, when milled in distilled water. By heating at 1673 K for 10 h in a flowing nitrogen atmosphere, both carbon and oxygen contents of the powder milled in toluene were decreased to the levels of as-received powder. The sample prepared with the whisker seeds had a coarse microstructure while the sample prepared from the powder milled in distilled water had a fine microstructure. The coarser microstructure sample showed the highest fracture toughness and the highest erosion rate while the finer microstructure sample showed the lowest erosion rate. Erosion rates of the samples in this study depended on the grain size more than the mechanical properties including hardness and the fracture toughness. Erosion occurred mainly by grain dislodgment following intergranular fracture.

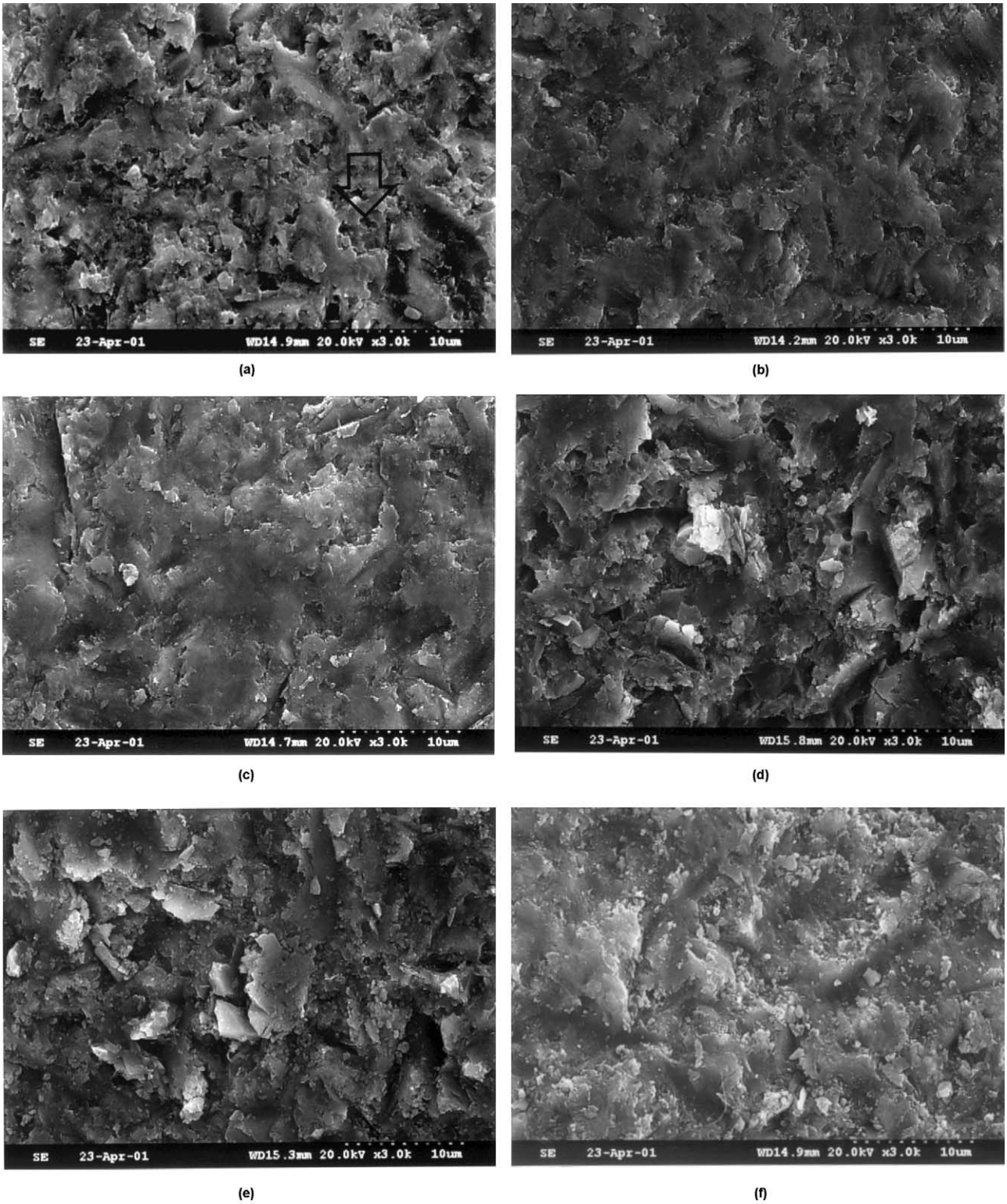

Fig. 6. FEG-SEM micrographs of eroded regions of samples: (a) sample C tested at RT, (b) sample FC at RT, (c) sample FW at RT, (d) sample C at 973 K, (e) sample FC at 973 K, (f) sample FW at 973 K.

Acknowledgements

This work is supported by NRL program of Korean Ministry of Science and Technology. Authors appreciate Mr. R. Fluch for the help with manuscript preparation.

References

[1] F.L. Riley, Silicon nitride and related materials, J. Am. Ceram. Soc. 83 (2) (2000) 245–265.
[2] S. Wada, Y. Kumon, The effects of impact angles of jet stream in the abrasive water jet cutting of Si_3N_4 ceramics, J. Ceram. Soc. Jpn. 101 (1993) 1297–1301.
[3] J. Pyzik, D.R. Beaman, Microstructure and properties of self-reinforced silicon nitride, J. Am. Ceram. Soc. 76 (1993) 2737–2744.
[4] Y. Zhang, Y.-B. Cheng, S. Lathabai, Influence of microstructure on the erosive wear behaviour of Ca α-sialon materials, J. Eur. Ceram. Soc. 21 (2001) 2435–2445.
[5] D.-M. Liu, J.-T. Lin, R.R.-R. Lee, Erosive wear behaviour in duophase Sialon composites, Ceram. Int. 24 (1998) 217–221.
[6] M. Marrero, J. Routbourt, Solid-particle erosion of in situ reinforced Si_3N_4, Wear 162–164 (1993) 280–284.
[7] R.W. Davidge, F.L. Riley, Grain-size dependence of the wear of alumina, Wear 186-187 (1995) 45–49.
[8] M. Dietz, H.-D. Tietz, Characterization of engineering ceramics by indentation methods, J. Mater. Sci. 25 (1990) 3731–3738.
[9] Y. Kameshima, A. Yasumori, K. Okada, XPS analysis of grinding solvent effect for surface state of wet ground silicon nitride powders, in: C. Galassi (Ed.), the Fourth Euroceramics, Vol. 1, Basic Science—Development in Processing of Advanced Ceramics—Part I, Gruppo Editoriale Faenza Editrice S.p.A, Italy, 1996, pp. 83–88.
[10] C. Wang, H. Emoto, M. Mitomo, Nucleation and growth of silicon oxynitride grains in a fine-grained silicon nitride matrix, J. Am. Ceram. Soc. 81 (5) (1998) 1125–1132.
[11] H. Eomoto, M. Mitomo, C.-M. Wang, H. Hirotsuru, T. Inada, Fabrication of silicon nitride–silicon oxynitride in-situ composites, J. Eur. Ceram. Soc. 18 (1998) 527–533.
[12] A.G. Evans, M.E. Gulden, M. Rosenblatt, Impact damage in brittle materials in the elastic-plastic response regime, Proc. Roy. Soc. London, Ser. A 361 (1978) 343–365.